Kent Academic Repository

Wood, N.D., Howe, R.A., Newport, Robert J. and Faber, J. (1988) *The Structure Of Molten Nickel Iodide.* Journal of Physics C: Solid State Physics, 21 (4). pp. 669-680. ISSN 0022-3719.

Downloaded from
https://kar.kent.ac.uk/16005/ The University of Kent's Academic Repository KAR

The version of record is available from
https://doi.org/10.1088/0022-3719/21/4/005

This document version
UNSPECIFIED

DOI for this version

Licence for this version
UNSPECIFIED

Additional information

Versions of research works

Versions of Record
If this version is the version of record, it is the same as the published version available on the publisher's web site. Cite as the published version.

Author Accepted Manuscripts
If this document is identified as the Author Accepted Manuscript it is the version after peer review but before type setting, copy editing or publisher branding. Cite as Surname, Initial. (Year) 'Title of article'. To be published in *Title of Journal* , Volume and issue numbers [peer-reviewed accepted version]. Available at: DOI or URL (Accessed: date).

Enquiries
If you have questions about this document contact ResearchSupport@kent.ac.uk. Please include the URL of the record in KAR. If you believe that your, or a third party's rights have been compromised through this document please see our Take Down policy (available from https://www.kent.ac.uk/guides/kar-the-kent-academic-repository#policies).

J. Phys. C: Solid State Phys. **21** (1988) 669–680. Printed in the UK

The structure of molten nickel iodide

N D Wood†, R A Howe†, R J Newport‡ and J Faber Jr§
† Department of Physics, University of Leicester, Leicester LE1 7RH, UK
‡ Physics Laboratory, University of Kent, Canterbury, Kent CT2 7NR, UK
§ IPNS, Argonne National Laboratory, Argonne, IL 60439, USA

Received 29 July 1987

Abstract. The structure of molten NiI_2 has been investigated by measuring the intensity of neutron scattering from isotopically enriched samples. The experiments were undertaken at the Intense Pulsed Neutron Source, Argonne, and employed time-of-flight techniques. The three partial structure factors and the corresponding radial distribution functions, relating to Ni–Ni, Ni–I and I–I correlations, have been determined from the experimental data. Aspects of the data analysis peculiar to pulsed sources are described and the detailed structural features of molten NiI_2 are presented in the context of other studies of 2:1 molten salts. The importance of ionicity and charge-transfer effects is discussed.

1. Introduction

In an earlier study (Newport *et al* (1985), subsequently referred to as I) the partial structure factors and associated radial distribution functions for molten nickel chloride were obtained from neutron diffraction studies of isotopically enriched samples. In general, the results resembled those obtained for molten zinc chloride (Biggin and Enderby 1981a) but detailed comparison revealed differences which cast doubt on the simple ion-size effect model and suggested that polarisation effects were important. The work presented here represents a continuation of this research and the choice of nickel iodide as the system to study has been made for a number of reasons.

The presence of nickel as the cation allows the opportunity of employing the isotopic substitution technique using the nickel species with the attendant advantages for sensitivity and conditioning that were described in I. In addition, the availability of well characterised, stable isotopes of the cation species enables one, uniquely, to undertake a detailed study of halides other than the chloride. The choice of iodine as the anion species can be justified in terms of the difference in polarisability between the chloride and iodide which for observations of polarisation effects must be a key factor. Furthermore, the scattering length of iodine is such as to enable a more accurate determination of the cation–cation correlation than has been obtained to date in such systems. Finally, solid nickel iodide is known to be structurally similar to solid nickel chloride (Wyckoff 1963), so any substantial differences between the structures of the two liquids can be interpreted as liquid state effects.

2. Experimental details

From a single neutron scattering measurement on a liquid containing two atomic species a and b in atomic concentrations c_a and c_b one can determine the total structure factor $F(Q)$ defined by

$$F(Q) = c_a^2 b_a^2 (S_{aa} - 1) + c_b^2 b_b^2 (S_{bb} - 1) + 2c_a c_b b_a b_b (S_{ab} - 1) \tag{1}$$

where b_a and b_b are the associated coherent neutron scattering lengths. S_{aa}, S_{bb} and S_{ab} are the partial structure factors which, by Fourier transformation, are directly related to the pair distribution functions $g_{\alpha\beta}(r)$ by

$$S_{\alpha\beta}(Q) = 1 + (4\pi n/Q) \int (g_{\alpha\beta}(r) - 1) r \sin Qr \, \mathrm{d}r \tag{2}$$

where α, β = a or b and n is the atomic number density.

Measurements of the neutron scattering intensity from three isotopically distinct samples of molten NiI_2 will yield three values for the total structure factor $F(Q)$ from which the three partial structure factors can be deduced. The samples used in this study where obtained by isotopic substitution of the nickel species with the enrichments and associated scattering lengths as detailed in table 1.

The samples were prepared as in I and contained in fused silica tubes of external diameter 10.0 mm and with a wall thickness of 1.0 mm. The choice of containment material was constrained by the corrosive nature of molten NiI_2. The samples were heated to a temperature of 830 ± 3 °C, some 30 degrees above their melting point, by means of a vanadium foil furnace. The intensity of neutron scattering was measured on the General Purpose Powder Diffractometer (GPPD) at the Argonne National Laboratory's Intense Pulsed Neutron Source. The neutron beam height was 25 mm. Time-of-flight analysis was employed for data collected, simultaneously, in twelve groups of detectors placed at scattering angles, $2\theta = -20°, +30°, \pm 45°, \pm 60°, \pm 75°, \pm 90°$ and $\pm 150°$ for counting periods of about 250 μA h (roughly equivalent to 20 h) per sample. Time channel widths of 80, 60, 45, 30, 25, 20 and 15 μs were used for the angles above, leading to a resolution $(\Delta Q/Q)$ at $Q = 2$ Å^{-1} of between 0.007 at 90° and 0.025 at 20°. Time focusing corrections were made for each detector within a group and data from the 'positive'-angle bank were analysed separately from data from the 'negative'-angle bank. Normalisation was made by reference to the measurement of neutron scattering from a vanadium rod. Corrections for sample attenuation, multiple, incoherent and container scattering were made in the manner described by Howells (1986).

Table 1. The isotopic enrichments and scattering lengths for the NiI_2 samples.

	Composition (at.%)				Effective coherent scattering lengths†	
Sample	^{Nat}Ni ($b = 1.03$)	^{60}Ni ($b = 0.282$)	^{62}Ni ($b = -0.87$)	^{Nat}I ($b = 0.528$)	$\bar{b}_{Ni}$ (10^{-12} cm)	$\bar{b}_I$ (10^{-12} cm)
'Nat' NiI_2	33.3	—	—	66.7	1.03	0.528
'62' NiI_2	1.1	—	32.3	66.7	−0.805	0.528
'Zero' NiI_2	0.5	24.3	8.5	66.7	0.00	0.528

† Sears (1984).

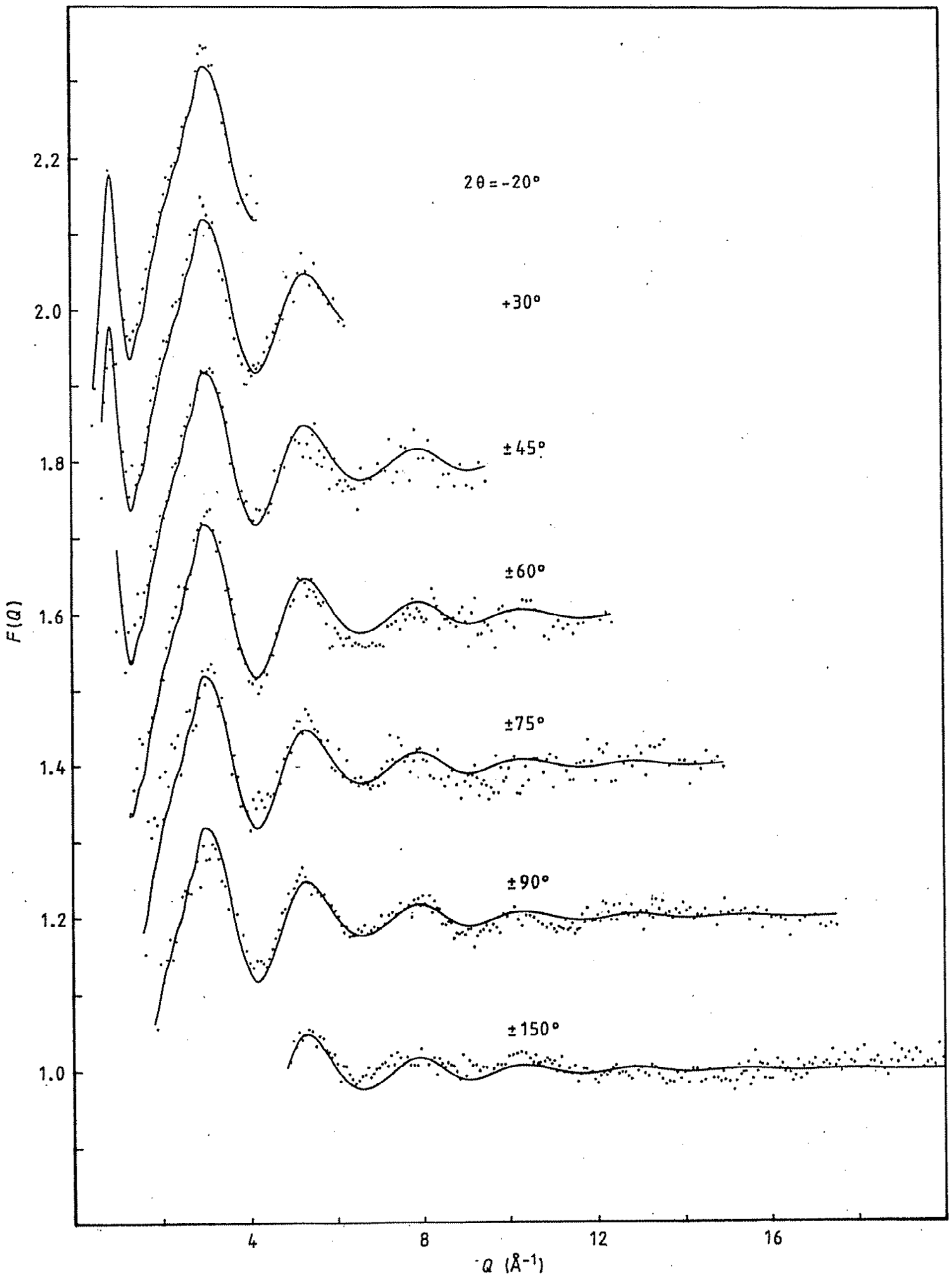

Figure 1. Natural NiI_2 $F(Q)$ data for each of the seven detector angles that contribute to the composite $S_{\alpha\beta}(Q)$. The points are experimental and the curves are derived from the back-transforms of the distribution functions shown in figure 5. Successive curves are displaced by 0.2.

There are distinct differences between the pulsed-source data analysis techniques used by Howells and those of constant-wavelength experiments. In particular, both attenuation and multiple scattering are wavelength-dependent.

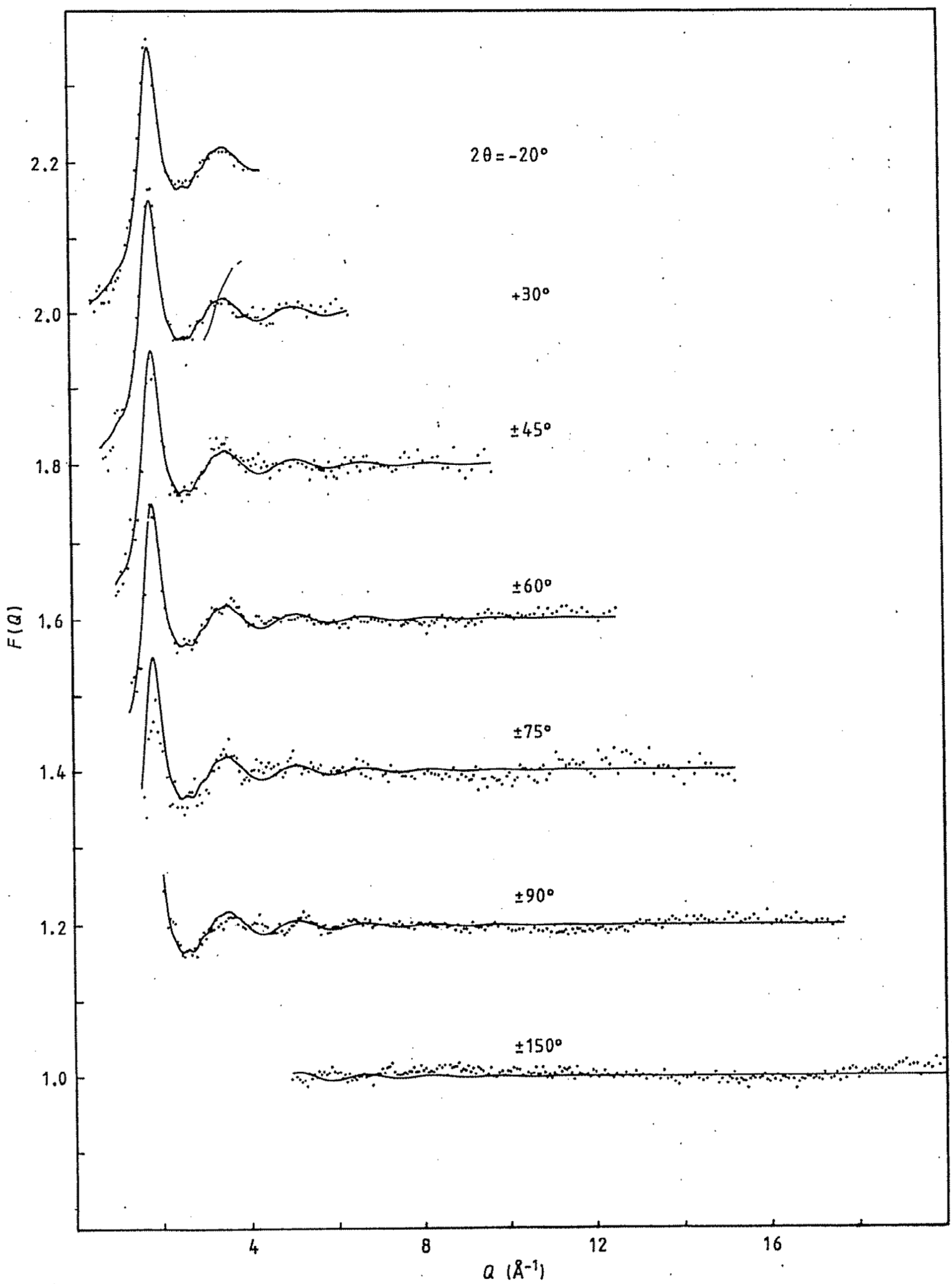

Figure 2. 'Zero' NiI_2 $F(Q)$ data (see the caption for figure 1).

The resulting $F(Q)$ data for each of the three samples are presented in figures 1 to 3 where the contribution from each of the seven counting angles can be compared. The positive- and negative-angle scattering banks showed excellent agreement and have been combined for the purposes of these figures.

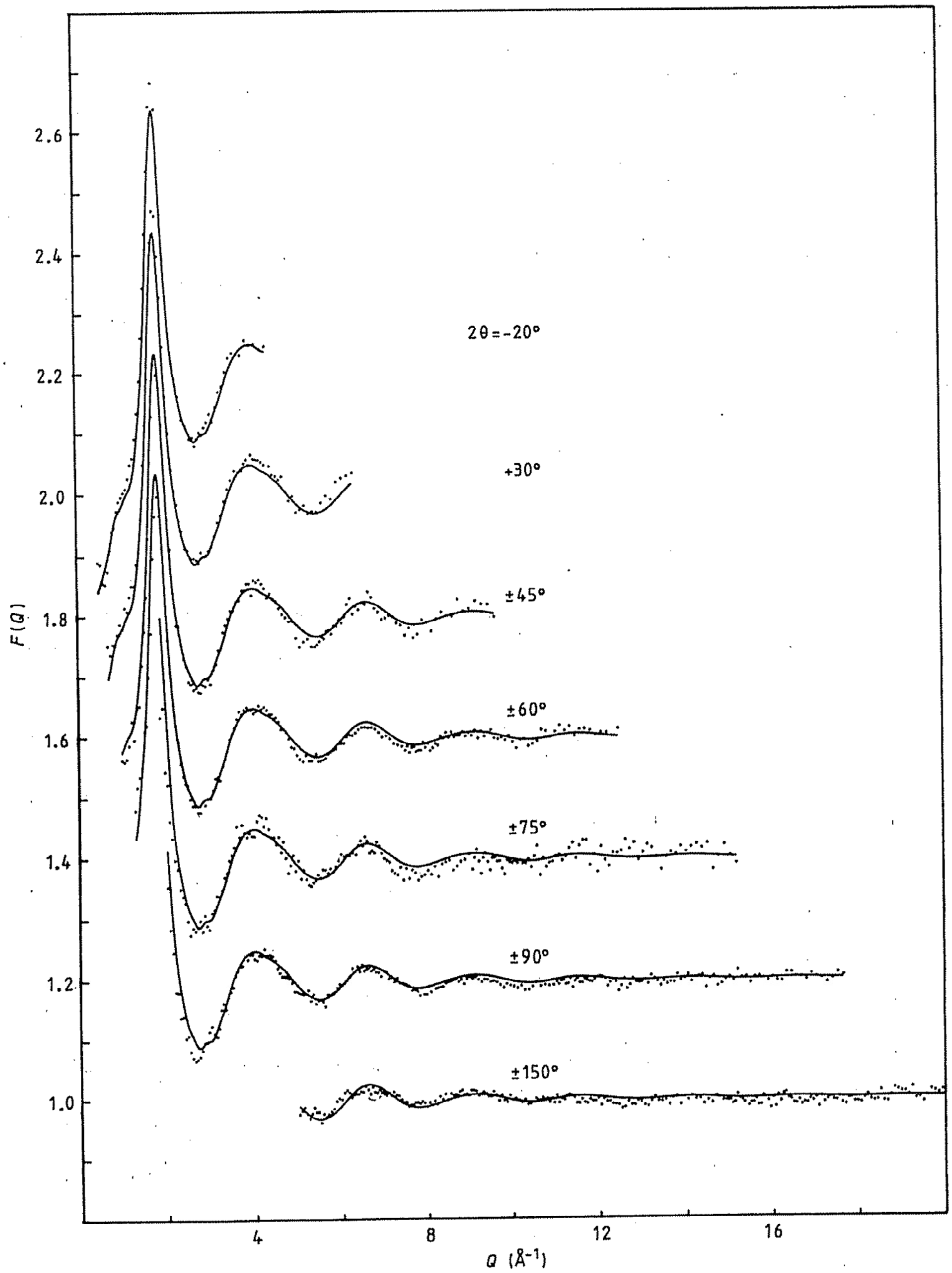

Figure 3. $^{62}NiI_2$ $F(Q)$ data (see the caption for figure 1).

3. Structure factors and radial distribution functions

Contributions to the three partial structure factors were obtained from the $F(Q)$ data for each of the individual counter banks by direct solution of the three simultaneous

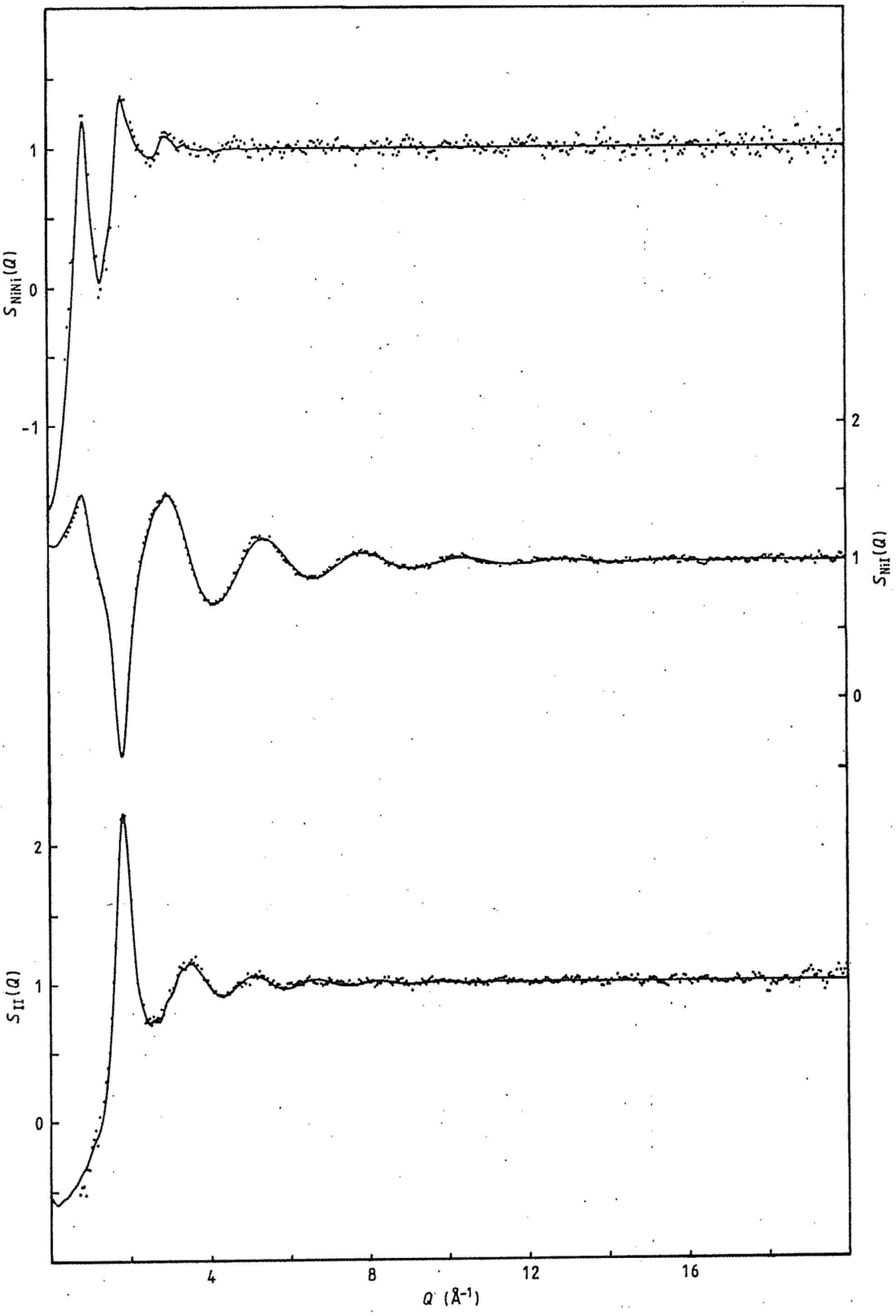

Figure 4. The partial structure factors for liquid $\mathrm{NiI_2}$. The points are the combined data sets for the seven detector angles and the curves are the back-transforms of the distribution functions shown in figure 5.

equations that result from the application of equation (1). For the isotopic substitutions of table 1, equation (1) yields

$$F(Q)\text{'Zero'} = 0.124(S_{II}(Q) - 1) \tag{3}$$

$$F(Q)\text{'62'} = 0.124(S_{II}(Q) - 1) + 0.072(S_{NiNi}(Q) - 1) - 0.189(S_{NiI}(Q) - 1) \tag{4}$$

$$F(Q)\text{'Nat'} = 0.124(S_{II}(Q) - 1) + 0.118(S_{NiNi}(Q) - 1) + 0.242(S_{NiI}(Q) - 1). \tag{5}$$

The anion–anion partial structure factor is obtained directly from the 'Zero' nickel data. Then, by substitution, two simultaneous equations were solved to produce the cation–cation and cation–anion factors. In contrast to the $NiCl_2$ case (see I), the coefficient of the Ni–Ni partial is comparable to that of the other terms and thus the experiment provides more detailed information on the cation structure.

In order to optimise the Fourier transform in equation (2), the data from the individual counter banks were combined to form a single data set which extends over the full range of momentum transfer covered by the experiment. The combination of the detector banks is not a trivial problem. In particular the resolution function is angle-dependent, although for liquid structure factors the breadth of the diffraction peaks is usually, as in this case, much greater than the resolution limit. To achieve the composite $S_{\alpha\beta}(Q)$ the contribution from each angle was interpolated onto a grid of equi-spaced Q-values with an interval of 0.02 $Å^{-1}$. At each Q-value, a weighted mean (in accord with counting statistics) was determined from the counters that contributed. For complete consistency, the contributing Q-range for each counter was held constant over the three samples. The resulting composite partial structure factors are presented in figure 4. The

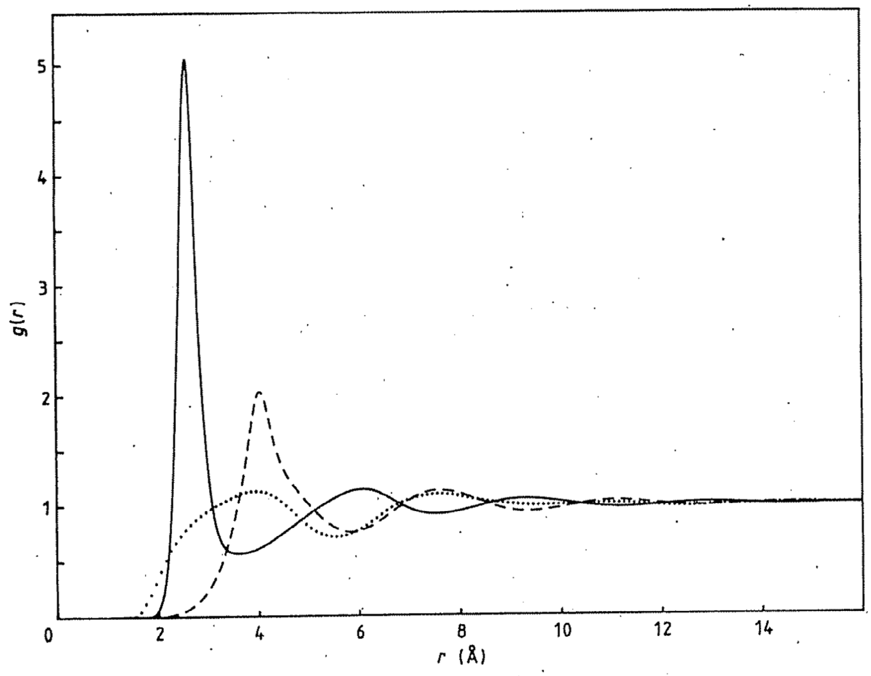

Figure 5. The radial distribution functions for liquid NiI_2: full curve, $g_{NiI}(r)$; broken curve, $g_{II}(r)$; dotted curve, $g_{NiNi}(r)$.

agreement between the data from the different-angle counter banks was satisfactory and an angle-dependent renormalisation was found to be unnecessary. The upper Q-limit was determined from the range of acceptable agreement between the $+150°$ and $-150°$ counter banks and is approximately 20 Å^{-1}.

The three partial structure factors are Fourier transformed to produced the radial distribution functions of figure 5. The procedure follows that detailed in I and the consistency of the transform is indicated in figures 1 to 3 where the full curves represent the back-transforms of the final radial distribution functions superimposed upon the original data. A summary of the structural parameters for molten NiI_2 are presented in table 2. The coordination numbers of β-type atoms about an α-type atom have been determined using the methods described by Waseda (1980): the first method is by integration of $4\pi r^2 g(r)$ to the first minimum following the principle peak; the second and third methods are based on the assumption that the functions $rg(r)$ and $r^2g(r)$ are symmetric about the first peak position; the fourth method is by extrapolation of the high-r side of the principle peak to the abscissa.

Amongst the more distinctive features of the data are the following.

(i) *The very large pre-peak at* $Q \simeq 0.9$ Å^{-1} *in the Ni–Ni partial structure factor.* This feature is indicative of intermediate-range order in the nickel species. The pre-peak was well resolved in the GPPD data and was substantiated by a subsequent, non-isotopic total $F(Q)$ measurement on the Liquids and Amorphous materials diffractometer (LAD) at the ISIS pulsed neutron source, Rutherford Appleton Laboratory, in which the data on the leading edge were extended to somewhat lower Q-values ($\simeq 0.15$ Å^{-1}). The feature was observed to occur at a Q-value that corresponds with a Bragg peak in the solid (GPPD data were also taken below the melting point) but was found to persist, essentially unchanged, to temperatures over 100 °C above the melting point which removes the possibility that the feature could derive from incomplete melting.

(ii) *The broad, extended principal peak in the Ni–Ni radial distribution function*, extending from the leading edge of the Ni–I peak to the trailing edge of the I–I peak. The shape of this feature is inconsistent with the usual, almost Gaussian features of liquid structure. Indeed, the data-reduction process suggested that the best fit of the back-transformation was achieved by a twin peak, with one maximum corresponding to the position of the Ni–I principal peak and the second in the same position as the I–I

Table 2. Structural parameters of liquid NiI_2.

Structural parameters		Ni–Ni	I–I	Ni–I
Position of the principal peak				
in $g_{\alpha\beta}(r)$	(Å)	3.9 ± 0.4	4.0 ± 0.1	2.58 ± 0.04
in $rg_{\alpha\beta}(r)$	(Å)	4.3	4.05	2.58
in $r^2g_{\alpha\beta}(r)$	(Å)	4.6	4.1	2.60
Position of first minimum in $g_{\alpha\beta}(r)$		5.6	5.8	3.6
Coordination of β-atoms around α				
in $g_{\alpha\beta}(r)$ by integration				
to first minimum in $g_{\alpha\beta}(r)$		5.3 ± 0.5	13.1 ± 1.0	4.2 ± 0.2
over $rg(r)$ symmetric		5.2	6.3	2.8
over $r^2g(r)$ symmetric		6.5	6.9	3.1
with high-r extrapolation		5.5	12.0	4.2

principal peak. However, given the possible errors in the numerical coefficients presented in equations (3), (4) and (5) and that the magnitude of this splitting is comparable with effects arising from truncation errors in the fourier transforms, the data are presented as a broad single peak.

(iii) *A marked dissimilarity between the anion and cation distribution functions* in contrast to the case for $NiCl_2$ and many other molten salts (Biggin and Enderby 1981a, b, Biggin *et al* 1984).

(iv) *An asymmetry of the shape of the principal peak in the I–I distribution.* The anion-anion structure resembles that of the $NiCl_2$ melt. The asymmetry of the principal peak in both salts yields a high value of 13 ± 1 for the nearest-neighbour coordination number obtained by integration of $4\pi r^2 g(r)$ to the first minimum. This is in contrast to values around half of this for the close-contact coordination numbers given by either of the symmetrisation methods (March and Tosi 1984).

4. Discussion

The crystalline form of the nickel halides has been described by Wyckoff (1963) as being of the $CdCl_2$ type. As discussed in I for $NiCl_2$, NiI_2 has a layered structure of cubic close-packed iodine ions with the nickel ions filling the octahedral sites between alternate layers thereby forming a rhombohedrally centred hexagonal structure themselves. Analysis of the melt data reveals that the sixfold coordination of iodine ions around each nickel ion is reduced to a value of 4.2 ± 0.2 in the liquid. A comparison of the liquid state coordination numbers and nearest-neighbour distances with their solid state counterparts is made in table 3.

As reported for $NiCl_2$ in I, the nickel ions in liquid NiI_2 are fourfold-coordinated and occupy tetrahedral sites in the anion structure. In a true tetrahedron, the ratio $R = r_{--}/r_{+-} = \sqrt{\frac{8}{3}} = 1.63$. In liquid NiI_2 the value is found to be 1.57 ± 0.04 from the peak positions of $r^2 g_{--}(r)$ and $r^2 g_{+-}(r)$. This suggests an arrangement that is fairly close to being truly tetrahedral.

A second similarity with liquid $NiCl_2$ lies in the halide structure. Both the chlorine and iodine ions occupy a densely packed structure with a large nearest-neighbour coordination number of 13 ± 1 for both salts. The iodine–iodine separation of 4.1 Å is close to that obtained by a simple rigid ion-size scaling of the 3.8 Å found for the chlorine–chlorine distance in molten $NiCl_2$.

Table 3. Comparison of the structures of solid and liquid NiI_2. $\bar{r}_{\alpha\beta}(r)$ is the peak position in $r^2 g_{\alpha\beta}(r)$ and $\bar{n}_{\alpha\beta}$ is the coordination number of β-atoms around an α-atom.

	Ni–Ni	I–I	Ni–I
Sum of ionic radii (Å)	1.38	4.32	2.85
Solid†			
$\bar{r}_{\alpha\beta}$ (Å)	3.89	3.89	2.75
$\bar{n}_{\alpha\beta}$	8	8	6
Liquid			
$\bar{r}_{\alpha\beta}$ (Å)	4.6 ± 0.4	4.1 ± 0.1	2.60 ± 0.04
$\bar{n}_{\alpha\beta}$	5.3 ± 0.5	13 ± 1	4.2 ± 0.2

† Wyckoff (1963).

The unique feature of molten NiI_2 is undoubtedly the form of the cation–cation radial distribution function. The broad first peak is dissimilar not only from $NiCl_2$ but from any other 2:1 molten chloride studied to date. The high-r region of this feature corresponds in position to the anion–anion peak (consistent with results for other 2:1 molten salts with small cations) but the degree of overlap with the principal peak of the cation–anion distribution is so large that its magnitude has scarcely diminished even at the position of the cation–anion main peak. This extensive penetration of the nickel species into the first coordination shell is without precedent and in view of the expected ionisation of these salts in the melt, namely $NiI_2 \leftrightharpoons Ni^{2+} 2I^-$ needs some explanation. A simple, Coulombic model would suggest that the doubly charged nickel ions, although small in size and thus well suited to interstitial siting in the iodine structure, would be strongly repelled from the first coordination shell around a nickel ion. Indeed, in a systematic investigation of the effect of changing the softness of the repulsive component of the inter-ionic potential in 2:1 molten salts using calculations based on the hypernetted-chain approximation, Copestake and Evans (see Biggin *et al* 1984) found that in every case they considered the cation–cation peak position was at significantly greater values of r than the corresponding anion–anion peak position.

Although the extent of the penetration is unique there are two other salt systems in which the cation–cation radial distribution function exhibits a broad first peak accompanied by the very rapid decay of $g_{NiNi}(r)$ to unity, which is the second characteristic of the Ni–Ni distribution. The first of these is molten CuCl where the features in the early data of Page and Mika (1971) have been confirmed by Eisenberg *et al* (1982). Numerous attempts have been made to explain these data. An Interpretation by Powles (1975) based on a molecular model has been critically examined by Gillan (1976) who concluded that the molecular view was unsatisfactory. Indeed, the evidence of electrical conductivity and the observed nuclear relaxation times (Boyce and Mikkelson 1977) are consistent with an ionic description. More recently, Ginoza *et al* (1987) have found that whilst chemical effects (Enderby and Neilson 1980) are significant in molten CuCl, the combined effects of partial ionicity and size difference between the ions are sufficient to provide a crude qualitative account of the structure. Furthermore, by adopting a partial charge-transfer model in which the effective charge is $Z = 0.16$ they conclude that the Cu ions resemble a one-component plasma.

Neutron scattering experiments on α-AgI (Howe *et al* 1985) reveal a cation–cation partial distribution function which, in common with CuCl and NiI_2, has a broad first peak and is lacking in any long-range order. Both CuCl and AgI are well known as salts that exhibit super-ionic behaviour and, in both cases, the mobile ion species is the cation. The similarity with NiI_2 would suggest that something closely related to super-ionicity is occurring in this system. Rovere and Tosi (1986) observe that the combination of fourfold coordination with low values of Z favours high mobility of the cation, the essence of their argument being that the cations can easily diffuse through such a low-coordinated structure under the influence of moderate Coulombic forces. A quasi-elastic neutron scattering study, again exploiting the unique opportunity presented by the availability of nickel isotopes, will be undertaken in an attempt to quantify the degree of mobility of the cations in molten NiI_2.

A more detailed comparison of molten NiI_2 with α-AgI reveals additional similarities. In α-AgI the anions form a body-centred cubic lattice through which the mobile cations move between tetrahedral sites (Parrinello *et al* 1983). The first peak of the anion–anion distribution function is made up of the first two coordination shells of the thermally disordered lattice containing 8 and 6 ions respectively. In NiI_2 also, this peak is asymmetric and shows a coordination number approaching 14. The value of the effective charge in α-AgI is accepted to be about 0.6, again small.

Finally, in describing the metal–non-metal transition in binary liquid systems containing a 3d transition metal, Enderby and Barnes (private communication) argue that the appropriate charge transfer will be determined by the energy difference Δ between the occupied hybridised ligand band and the empty d band, rather than by the very much larger Mott–Hubbard energy U. Their model is described principally within the context of data on molten nickel chalcogenides but is based on earlier, more general work on the solid state which include a study of the nickel halides (Zaanen *et al* 1985). The suggestion here is that the anion valence (ligand) band hybridises with the cation d band. Thus, whilst the Ni 4s states have been emptied as expected for a purely ionic system, much of that charge has gone into the hybridised d band. The ground state of the nickel ion has ligand admixtures and may be described as $d^8 + d^9L$, where L is the (delocalised) hole in the ligand band; photo-emission results have provided strong experimental support for this model (Hüfner 1985, Starnberg *et al* 1986). It must be borne in mind that the electronic structure calculations and photo-emission data referred to above all relate to solid NiI_2 and can only be of significant use in explaining liquid state behaviour if the local atomic arrangement is similar to that of the solid. Our structural data for the molten salt do show similarities with the solid, but it is also clear from table 3 that there are substantial differences. Nevertheless we feel that the solid state data give a good indication of likely liquid state processes. For NiI_2 then, this suggests that the charge on the nickel ion will be substantially reduced in the tetrahedral iodide environment. A transfer of charge by the above mechanism will be directly related to the electronegativity of the anion (see, e.g., Zaanen *et al* 1985) and the charge transfer for molten $NiBr_2$ should therefore be intermediate between that for the iodide and the chloride. Measurements of the structure of molten $NiBr_2$ will form the basis of a later paper where charge-transfer effects and structural trends through the nickel halides will be discussed further. Work is also in hand to measure the electrical conductivity of the nickel halides, which will provide further information of direct relevance to the problem.

In conclusion, the data suggest a model in which the small nickel ion occupies tetrahedral sites in a closely packed anion structure analogous to both $ZnCl_2$ and $NiCl_2$. In this system, however, the nickel ion is able to penetrate the first coordination shell of anions and the results suggest that the nickel ion is considerably more mobile in this material. A charge transfer markedly below that envisaged for a simple, doubly charged ion model is comparible with such a description.

Acknowledgments

We would like to thank the staff at the IPNS (Argonne), particularly Mr R Hitterman, for assistance with the diffraction experiment. We are grateful to Mr J S G Taylor for technical liaison on the furnace design, the Physics Department Workshop for construction of the furnace, and Mr P Gullidge of Bristol University for preparation of the isotopic samples. Thanks are also due to Dr W S Howells for advice on data reduction and assistance with the ISIS-LAD experiment. We acknowledge the continued support given to this work by the Science and Engineering Research Council and one of us (NDW) wishes to thank the University of Leicester for the award of a research Studentship.

References

Biggin S and Enderby J E 1981a *J. Phys. C: Solid State Phys.* **14** 3129
—— 1981b *J. Phys. C: Solid State Phys.* **14** 3577
Biggin S, Gay M and Enderby J E 1984 *J. Phys. C: Solid State Phys.* **17** 977
Boyce J B and Mikkelson J C Jr 1977 *J. Phys. C: Solid State Phys.* **10** L41
Enderby J E and Neilson G W 1980 *Adv. Phys.* **29** 323
Eisenberg S, Jal J F, Dupuy J, Chieux P and Knoll W 1982 *Phil. Mag.* A **46** 195
Gillan M J 1976 *J. Phys. C: Solid State Phys.* **9** 2261
Ginoza J, Nixon J H and Silbert M 1987 *J. Phys. C: Solid State Phys.* **20** 1005
Howe M A, McGreevy R L and Mitchell E W J 1985 *Z. Phys.* B **62** 15
Howells W S 1986 *Rutherford Appleton Laboratory Report* RAL-86-042
Hüfner S 1985 *Solid State Commun.* **53** 707
March N H and Tosi M P 1984 *Coulomb Liquids* 1st edn (London: Academic)
Newport R J, Howe R A and Wood N D 1985 *J. Phys. C: Solid State Phys.* **18** 5249
Page D I and Mika K 1971 *J. Phys. C: Solid State Phys.* **4** 3034
Parrinello M, Rahman A and Vashishta P 1983 *Phys. Rev. Lett.* **50** 1073
Powles J G 1975 *J. Phys. C: Solid State Phys.* **8** 895
Rovere M and Tosi M P 1986 *Rep. Prog. Phys.* **49** 1001
Sears V F 1984 *Atomic Energy of Canada Ltd Report* AECL-8490
Starnberg H I, Johnson M T and Hughes H P 1986 *J. Phys. C: Solid State Phys.* **19** 2689
Waseda Y 1980 *Structure of Non-Crystalline Materials: Liquids and Amorphous Solids* 1st edn (London: McGraw-Hill)
Wyckoff R W G 1963 *Crystal Structures* 2nd edn, vol 1 (New York: Interscience)
Zaanen J, Sawatzky G A and Allen J W 1985 *Phys. Rev. Lett.* **55** 418